MOBILE HTS SQUID SYSTEM FOR EDDY CURRENT TESTING OF AIRCRAFT

H.-J. Krause, R. Hohmann, H. Soltner, D. Lomparski, M. Grüneklee,
M. Banzet, J. Schubert, W. Zander, Y. Zhang, W. Wolf, H. Bousack,
A.I. Braginski
ISI, Forschungszentrum Jülich GmbH (KFA)
52425 Jülich, Germany

M.L. Lucía
Dpto Fisica Aplicada III, Universidad Complutense
Madrid 28040, Spain

E. Zimmermann, G. Brandenburg, U. Clemens, H. Rongen, H. Halling
ZEL, Forschungszentrum Jülich GmbH (KFA)
52425 Jülich, Germany

M.I. Faley, U. Poppe
IFF, Forschungszentrum Jülich GmbH (KFA)
52425 Jülich, Germany

H. Buschmann, G. Spörl, A. Binneberg
Institut für Luft- und Kältetechnik (ILK)
01309 Dresden, Germany

M. Junger
Rohmann GmbH
76277 Frankenthal, Germany

INTRODUCTION

In Non-Destructive Evaluation (NDE), eddy current techniques are commonly used for the detection of hidden material defects in metallic structures. Conventionally, one works with an excitation coil generating a field at a distinct frequency. The eddy currents are deviated by materials flaws and the resulting distorted field is sensed by a secondary coil. Because of the law of induction, this technique has its limitations in the low frequency range. This leads to a decrease of the Probability of flaw Detection (POD) in larger depths.

SQUID sensors are particularly well suited to be used as magnetic field sensors in NDE applications because of their high magnetic flux sensitivity which results in high field

Review of Progress in Quantitative Nondestructive Evaluation, Vol 16
Edited by D O. Thompson and D.E Chimenti, Plenum Press, New York, 1997

sensitivity together with good spatial resolution [1,2]. In conjunction with a well optimized flux locked loop electronics, SQUID systems are endowed with a very large dynamic range and high linearity. This is a prerequisite for the quantitative evaluation of the of magnetic field distributions, i.e. the solution of the inverse problem to unambiguously identify the flaw [3].

In a joint German R&D project, six partners are determined to evaluate the capabilities of SQUID sensors for use in eddy current testing of aircraft and to develop a demonstration device: Rohmann GmbH (small company developing and manufacturing standard eddy current equipment), Daimler Benz Aerospace Airbus (aircraft industry), Deutsche Lufthansa (aircraft operator), ILK Dresden (small company specialized in cryostats, cryogenic components and cooling devices), University of Gießen and Research Center Jülich.

Liquid nitrogen cooled SQUIDs can be used as extremely sensitive magnetic field sensors in practical applications because of the less stringent cooling requirements compared to LTS SQUIDs. To insure operation in any orientation, either specially designed cryostats can be applied [4] or machine coolers can be used. Machine coolers may lead to problems for SQUID operation due to electromagnetic interference by the compressor or moving parts in the cold end, vibrations which indirectly lead to EMI due to tilting of the SQUID in the geomagnetic field, or due to instability of the temperature. All these influences may have a negative effect on SQUID performance [5,6] and have to be dealt with [7]. This paper will focus on the performance of dc and rf SQUIDs, operated with a portable cryostat, and its application to NDE.

EXPERIMENTAL

The system consists of a SQUID chip and coupling circuit integrated with a portable cryostat, the SQUID readout electronics, the eddy current excitation coil arrangement (cf. Fig. 1), the lock-in detection, and a nonmagnetic scanning table for movement of the sensor relative to the sample.

SQUIDs and electronics: The SQUIDs integrated with the cryostat have already been described elsewhere. Briefly, rf washer SQUID magnetometers [8] with a field resolution of about 120 fT/√Hz and dc SQUID gradiometers [9] with a gradient field sensitivity of 750 fT/(√Hz·cm) and a baseline of 6 mm were used. The resolution data refer to the white noise region measured in magnetically shielded environment. The rf magnetometers were operated with a digital signal processor controlled flux-locked loop electronics [10,11], the dc gradiometers with a commercial electronics.

Cryostat: The cryostat can be operated in any orientation. Fig. 2 shows a cross section of it. The SQUID is mounted on the inside wall of a copper hood in the vacuum space of the cryostat. The hood is screwed to the copper cold end, which is in direct contact with liquid nitrogen on its rear side during normal operation and is cooled by thermal conduction via the inner copper wall while in the inverted orientation. The hood is thermally shielded against its surroundings by several layers of superinsulation (not shown in Fig. 2). The distance of the SQUID to the outer surroundings is about 1 cm. A charcoal reservoir ensures the preservation of the vacuum against small leaks and degassing during operation. After mounting the SQUID, the vacuum space is evacuated and the cryostat is filled half with 0.25 l of liquid nitrogen. The filling procedure takes about 20 minutes.

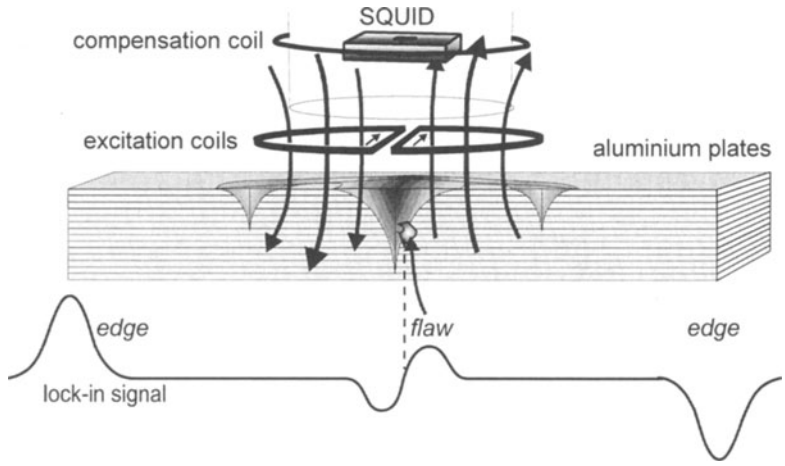

Figure 1. Principle of the eddy current technique used for our SQUID systems. A double-D configuration of the excitation coils is used to ensure a minimum field at the SQUID in the case of no flaw inside the structure.

Eddy Current Excitation: For the generation of eddy currents in the sample, a double-D configuration of induction coils was used [12]. This setup yields a minimum excitation field at the SQUID location. The differential arrangement ensures that only distortions of the magnetic field are sensed, due to deviations of the eddy currents inside the metallic structure by inhomogeneities like flaws.

Lock-in Detection: A digital lock-in technique was used to detect signals from the samples at the eddy current frequency, typically in the range from 20–30 Hz. Since a digital signal processor (DSP) is controlling the flux locked loop for the rf SQUIDs, the eddy current frequency generation and the lock-in procedure was synchronized with the DSP clock. Digital lock-in is known to be more accurate than analog lock-in especially at low frequencies because it operates drift-free and digital filters without phase distortions can be implemented. By dividing the flux-locked loop frequency, the eddy current frequency which is used to drive a current source for the excitation coil is derived. The SQUID signal

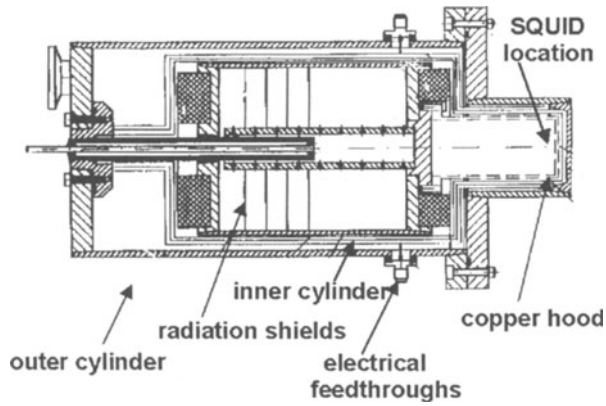

Figure 2. Cross section of the cryostat used for orientation independent SQUID operation. The SQUID is located inside the copper hood for electromagnetic shielding and thermal grounding to the cold plate.

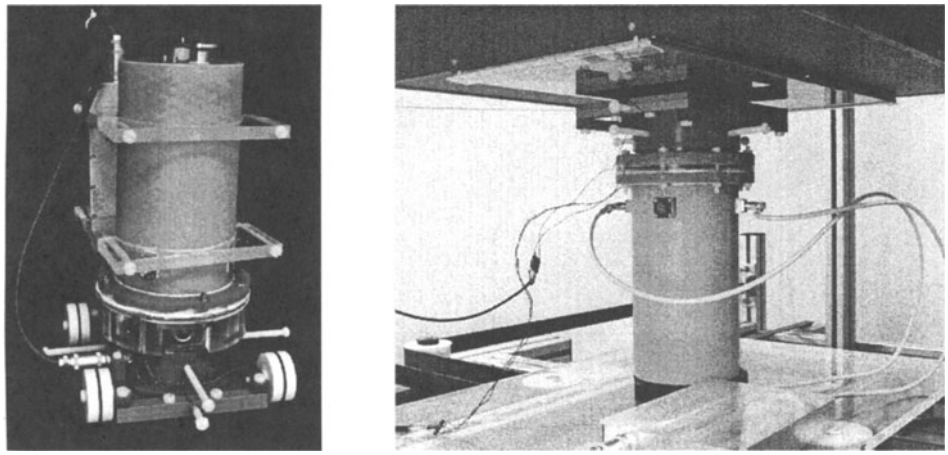

Figure 3. a) Mobile HTS System equipped with eddy current excitation coils and with wheels for manual movement, b) Operation of the mobile SQUID, mounted upside down on the belt-driven x-y-stage. The stack of aluminum plates being scanned is affixed overhead.

digitally supplied by the FIFO is then multiplied by the excitation sine wave and low-pass filtered to arrive at the lock-in signal.

Scanning Table: To investigate samples in NDE, a scanning table was constructed using non-magnetic materials. It allows the displacement of samples in two orthogonal directions with a belt-driven scanning stage underneath a stationary cryostat with a SQUID inside or the movement of the sensor system integrated with the movable cryostat underneath the sample to be investigated.

RESULTS

The minimum temperature after filling the cryostat with liquid nitrogen is about 78.3 K in the normal position or 78.8 K in the inverted position, with a temperature stability in the range of 10 mK for both positions. The temperature values describing the cooling power in Table I were determined in the normal position and the overhead position by dissipating electrical energy at the copper hood and measuring the corresponding temperature increase.

For both orientations, the temperature can be described with linear relationships to the cooling power P (in Watts):

$$\text{normal orientation:} \quad T(P) = 77.8\ \text{K} + 0.7\ \text{K} \cdot (P/\text{W})$$
$$\text{overhead orientation:} \quad T(P) = 78.8\ \text{K} + 1.4\ \text{K} \cdot (P/\text{W}).$$

Table I. Temperatures at the cold head of the cryostat attained with heat loads of 0 W, 1 W, 2 W, and 3 W for two different orientations.

Orientation	0 W	1 W	2 W	3 W
normal	77.8 K	78.5 K	79.2 K	79.9 K
overhead	78.8 K	80.2 K	81.6 K	82.6 K

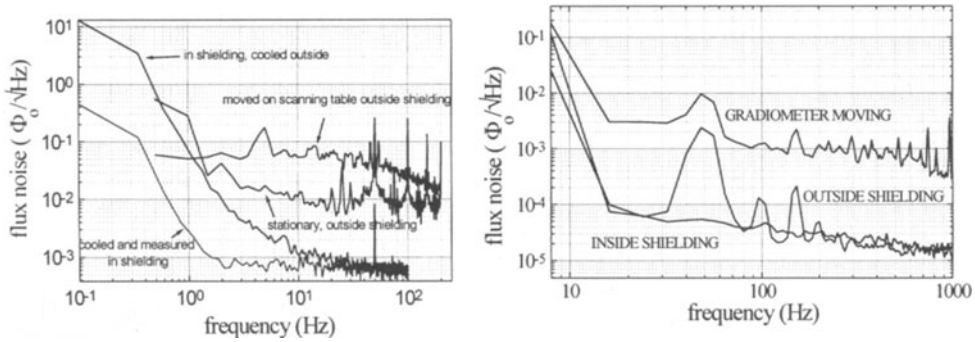

Figure 4. a) Field resolutions of the rf washer SQUID operated by the portable cryostat for four different situations, gradually approaching the most realistic case of a SQUID moved in unshielded environment on a scanning table, b) Flux noise of the dc SQUID gradiometer measured inside shielding without bias reversal and outside shielding. An increase of the white flux noise is observed during the movement.

Assuming a cooling power for the SQUID of 0.2 W, even in the overhead position the temperature will just be 79 K, which is an acceptable value for SQUID operation. The operation time of this cryostat is about 8 hours in the normal orientation and 7 hours in the overhead orientation. The cryostat can always be refilled to reach the end temperature without additional external pumping, if the temperature has not risen above about 200 K.

Fig. 4a shows the field resolution of the rf washer-SQUID integrated with the portable cryostat in four different situations. If the SQUID is cooled and measured inside magnetic shielding, the white noise is about $8 \cdot 10^{-4}$ $\phi_0/\sqrt{\text{Hz}}$ and the 1/f noise starts at only 2 Hz. This noise value is to be compared to the noise of the SQUID inside an ordinary liquid nitrogen dewar which is about 10 times smaller [8]. The cooling of the SQUID outside magnetic shielding before the measurement inside leads to an increase of the 1/f corner frequency to 10 Hz but leaves the white noise level unaffected. If the cooling and measuring procedures are performed outside the shielding, a white noise level higher by one order of magnitude is measured, due to the environmental noise in the laboratory. When moving the SQUID system with the scanning table, further increase of the flux noise by again one order of magnitude up to $7 \cdot 10^{-2}$ $\phi_0/\sqrt{\text{Hz}}$ was observed. This amounts to a magnetic field noise of the moving SQUID magnetometer of about 100 pT/√Hz, three orders of magnitudes higher than the intrinsic SQUID noise. This strong increase of noise is understood fairly well and can be avoided as will be discussed below. The noise did not depend on the orientation of the cryostat. The temperature stability during movement is about 10 mK.

We also integrated dc gradiometers with the cryostat and performed similar noise measurements inside and outside magnetic shielding. Fig. 4b shows the results. Inside shielding a white noise level of about $2 \cdot 10^{-5}$ $\phi_0/(\sqrt{\text{Hz}} \cdot \text{cm})$ is attained at frequencies of about 1000 Hz. A gradual increase is observed down to 20 Hz, which we attribute to the fact that we did not use any bias reversal scheme for this measurement. The stationary measurement outside shielding does not result in an overall increase in noise as in the case of the rf SQUID magnetometer (see Fig. 4a) but only at the line frequency and its harmonics an additional contribution is observed. When moving the dc gradiometer in the geomagnetic field, the white flux noise increases by more than one order of magnitude, similar to but not as strong as in the case of the SQUID magnetometer.

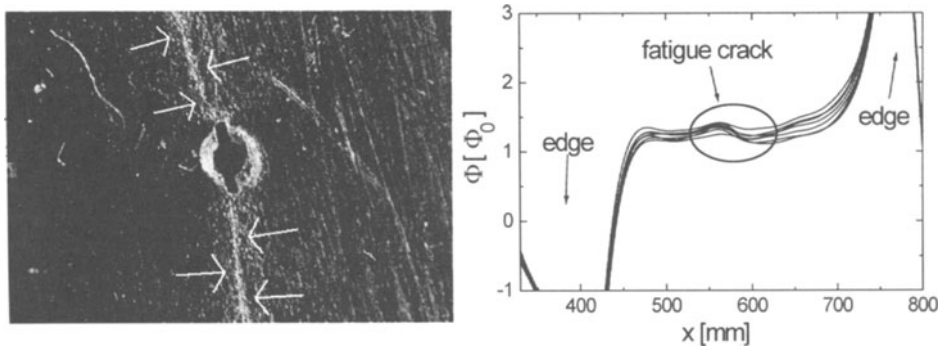

Figure 5. a) Fatigue crack (white arrows) in an aluminum plate induced by weakening one location by a hole of about 1 mm in diameter and stretching the plate several times (courtesy DASA Bremen, Germany, # DASA SQUID-ER001). b) Eddy current signal of the fatigue crack shown left, measured with moving rf magnetometer. The different traces correspond to different positions of the sensor in the horizontal direction normal to the x direction. The signal is dominated by the effects of the finite extension of the plates (edge effects).

To apply this system to the detection of flaws in structures relevant for aircraft inspection, we simulated a fatigue crack in an aluminum plate (width 160 mm) by weakening it at some point by a small bore hole and stretching the plate several times. A fatigue crack with a length of 43 mm developed, see Fig. 5. It was buried under four intact layers of aluminum with a thickness of 1.5 mm. The rf SQUID system was moved underneath this stack and scanned it magnetically with the eddy current technique. These measurements were performed outside any magnetic shielding.

Fig. 5b shows the result of this scan after lock-in evaluation at the eddy current frequency of 20 Hz. The most dominant signals arise from the edges of the aluminum plates. The lock-in signal clearly shows the expected differential signature originating from the flaw, thus demonstrating the detection of the flaw under the four intact layers of aluminum. The different traces correspond to different positions of the sensor in the horizontal direction normal to the x direction.

Fig. 6 depicts the equivalent measurement with a stack totaling 8 aluminum plates using a stationary dc gradiometer with gradiometric flux transformer [8] and moving the sample. The fatigue crack is easily identified through seven flawless layers.

DISCUSSION

To our knowledge, for the first time a movable HTS SQUID system for eddy current NDE outside magnetic shielding is presented, using a liquid nitrogen cryostat operating independent of orientation. The results shown in Figs. 5 and 6 clearly indicate that it is possible to obtain relevant results for aircraft testing with this system, although the flux noise increases significantly as compared to the case of the system being operated in a magnetically shielded dewar. This decrease in sensitivity has several origins. First, already inside shielding, one order of magnitude was lost. We attribute this effect to the influence of the abundance of metal parts close to the SQUID (see Fig. 2). Varpula and Poutanen [13]

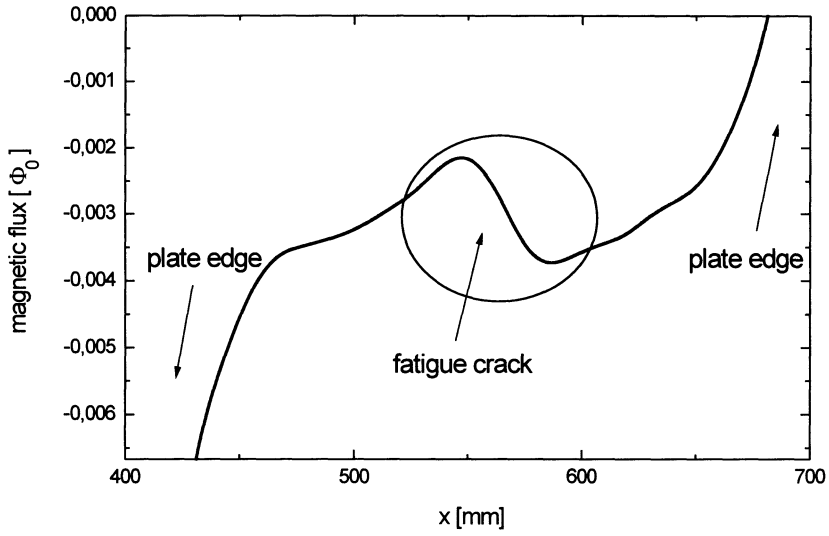

Figure 6. Eddy current signal of the fatigue crack shown in Fig. 5a, hidden underneath 7 flawless aluminum plates (total material thickness 12 mm), as measured using a stationary dc gradiometer with gradiometric flux transformer. The differential flaw signal clearly shows up between the strong signals originating from the edges.

have calculated the magnetic field due to the thermal motion of charge carriers in materials. According to their theory, already small metal parts lead to a magnetic field noise of several hundred fT/Hz close by. This can account for the increase of the white noise floor in Fig. 4 for the most favorable case shown there. This effect can be reduced by a proper choice of materials for the construction of the cold head, in particular the use of sapphire as a heat conducting material instead of copper. However, the environmental noise which dominates the system noise during stationary operation outside magnetic shielding, in the laboratory environment, can only be suppressed using a gradiometric sensor. The increase during movement may originate from sensor vibrations, from the motion of flux lines in the superconducting YBCO films, or from eddy currents generated in the copper by power line and other low-frequency fields. Recent work [7] with a new integration scheme, using a sapphire cold finger for planar rf gradiometers [14] operated with a Joule-Thomson cryocooler, demonstrates clearly that even during movement, the sensitivity of the SQUID is only weakly impaired. This leaves the last explanation as the most probable.

The recent success in suppression of the motion-induced SQUID noise [7], in combination with other advantages like high linearity and high dynamic range, make HTS SQUID very attractive sensors for eddy current NDE applications. Future work will include the improvement of the system regarding reliability and handling and its application for testing of aircraft structures. The large stand-off between SQUID and room temperature which is to be reduced. In addition, the eddy current excitation and sensor arrangement is to be adapted to the specific flaw detection problem.

ACKNOWLEDGMENTS

Helpful discussions with Ch. Heiden, M. Mück and M. v. Kreutzbruck (University of Gießen), J. Rohmann (Rohmann GmbH), W.B. Klemmt (DASA) and F. Schur (Lufthansa) are gratefully acknowledged.

This work was supported by the German BMBF under Grant No. 13 N 6682.
M.L. Lucía acknowledges financial support from DGICYES, Spain.

REFERENCES

1. J.P. Wikswo, IEEE Trans. Appl. Supercond. 5, 74 (1995).
2. C. Carr, M.E. Walker, D. McA. Mc Kirdy, G.B. Donaldson, „Advances in the use of LTS and HTS SQUIDs in electromagnetic NDE“, in this volume.
3. J.P. Wikswo, „The Magnetic Inverse Problem for NDE“, in: *SQUID Sensors: Fundamentals, Fabrication and Applications,* H. Weinstock, Ed., Kluwer Academic Publishers, Dordrecht, The Netherlands, in press.
4. R. Hohmann, M.L. Lucía, H. Soltner, H.-J. Krause, W. Wolf, H. Bousack, M.I. Faley, G. Spörl, and A. Binneberg, "Integration of HTS SQUIDs with portable cooling devices for the detection of materials defects in non-destructive testing", to be published in *Cryocoolers* 9, Proceedings of the 9th International Cryocooler Conference, 1996.
5. H.J.M. ter Brake, H.J. Holland, and H. Rogalla, "Stirling cooler magnetic interference measured by a High-T_c SQUID mounted on the cold tip", ibid.
6. N. Khare and P. Chaudhari, Appl. Phys. Lett. 65, 2353 (1994).
7. R. Hohmann H.-J. Krause, H. Soltner, Y. Zhang, C.A. Copetti, H. Bousack, A.I. Braginski, M.I. Faley, "HTS SQUID System with Joule-Thomson Cryocooler for Eddy Current Nondestructive Evaluation of Aircraft Structures", to be published in: IEEE Trans. Appl. Supercond., June 1997.
8. Y. Zhang, M. Mück, K. Herrmann, J. Schubert, W. Zander, A.I. Braginski, and C. Heiden, IEEE Trans. Appl. Supercond. 3, 2465 (1993).
9. M.I. Faley, U. Poppe, K. Urban, H.-J. Krause, H. Soltner, R. Hohmann, D. Lomparski, R. Kutzner, R. Wördenweber, H. Bousack, A.I. Braginski, V. Y. Slobodchikov, A. V. Gapelyuk, V. V. Khanin, Y. V. Maslennikov , *DC-SQUID Magnetometers and Gradiometers on the Basis of Quasiplanar Ramp-Type Josephson Junctions*, to be published in: IEEE Trans. Appl. Supercond., June 1997.
10. E. Zimmermann, G. Brandenburg, U. Clemens, and H. Halling, "Kompensationsregelung für extrem nichtlinearen Sensor mit digitalem Signalprozessor", in: *DSP Deutschland'95*, Design und Elektronik, Munich, 1995.
11. E. Zimmermann, G. Brandenburg, U. Clemens, H. Rongen, H. Halling, H.-J. Krause, R. Hohmann, H. Soltner, D. Lomparski, M. Grüneklee, K.-D. Husemann, H. Bousack, A.I. Braginski, "HTS SQUID Magnetometer with Digital Feedback Control for NDE Applications", in this volume.
12. Y. Tavrin, H.-J. Krause, W. Wolf, V. Glyantsev, J. Schubert, W. Zander, and H. Bousack, Cryogenics 36, 83 (1996).
13. T. Varpula and T. Poutanen, J. Appl. Phys. 55, 4015 (1984).
14. Y. Zhang, H. Soltner, H.-J. Krause, E. Sodtke, W. Zander, J. Schubert, M. Grüneklee, D. Lomparski, M. Banzet, H. Bousack, A.I. Braginski, "Planar HTS Gradiometers with Large Baseline", to be published in: IEEE Trans. Appl. Supercond., June 1997.